

Synthesis, Characterization, Thermal Properties Study and Analytical Efficiency of (Epoxy Resin-Poly Aniline) Nanomagnetic Semi IPNs

¹Samia Mezhr Merdas, ²Salah Sh. Al-luaibi and ¹Sajid Hassan Guzar

¹Department of Chemistry, College of Science, University of Thi-Qar, Nasiriyah, Iraq

²Department of Chemistry, College of Science, University of Basra, Basra, Iraq

Abstract: Nanomagnetic semi-Interpenetrating Polymer Networks (NM semi IPNs) derived from cured epoxy with amine hardener and polyaniline was synthesized by sequential polymerization in the presence of Fe₃O₄ nanomagnetic particles. The chemical structure and surface morphology of NM semi IPNs resin nanoparticles were characterized by Fourier Transform Infrared spectroscopy (FTIR), Scanning Electron Microscopy (SEM) and Transmission Electron Microscopy (TEM). The thermal properties of (NM semi IPNs) have been evaluated by Thermogravimetric Analysis (TGA) and Differential Scanning Calorimetric (DSC). Adsorption of Cu²⁺, Pb²⁺ and Cd²⁺ was investigated under different conditions such as pH and time using flameless atomic absorption spectroscopy. The adsorption studies were evaluated by using Langmuir and Freundlich isotherms.

Key words: Semi IPNs, nanomagnetic, adsorption studies, DSC, TEM, TGA

INTRODUCTION

Polymer composites especially, the Interpenetrating Polymer Networks (IPNs) have been paid more attention in recent years because of their excellent properties, e.g., light weights, high mechanical strength, high wear resistance, good thermal stability, good chemical resistance, etc. (Frisch *et al.*, 1983; Ramis *et al.*, 2001; Cristea *et al.*, 2009) IPNs are polymer alloys which consist of two or more polymers in a network form and held together by permanent entanglements with only occasional covalent bonds between the chains of the two different types of polymers (Yu *et al.*, 1999; Sperling and Mishra, 1996). Because of the synergetic effect induced by forced compatibility of individual components, IPN composites show excellent thermal stability and mechanical properties compared with those of single components (Sperling and Mishra, 1996; Raymond and Bui, 1998; Tsumura *et al.*, 1998; Yuhong *et al.*, 2010; Ramis *et al.*, 2001). Among the materials science, nanoparticles and nanocomposites have received a great deal of attention from scientists, due to their small sizes and related unique properties (Raymond and Bui, 1998; Tsumura *et al.*, 1998). Nanocomposite materials formed by metal nanoparticles that appropriately incorporated into the polymer matrix were found to be very significant due to their diversity in electrical, catalytic and optical properties. These diversities have potential applications in the fields of electronic, photonic, catalysis and bioengineering (Yuhong *et al.*, 2010) magnetite (Fe₃O₄)

combined with polymers/nanocomposites has unique multifunctional properties for materials such as small sizes, biocompatibility, low toxicity and superparamagnetism which is applied in medical fields and magnetic recording media (Ramis *et al.*, 2001; Qin *et al.*, 2006; Radhakrishnan *et al.*, 2001; Heath, 1999; Agarwal *et al.*, 2011; Unal *et al.*, 2010). Therefore, magnetite plays a potential key role for providing the desired electrical and magnetic properties in the final composite. This study focused about using nanomagnetic interpenetrating polymer networks derived from cured epoxy with amine hardener and poly aniline to remove heavy metals such as Cu²⁺, Pb²⁺ and Cd²⁺ from waste water.

MATERIALS AND METHODS

Experimental: Aniline, Potassium Iodate (KIO₃), Sulfuric acid (H₂SO₄), Epoxy resin, triethylenetetramine, Iron (III) Chloride Hexahydrate (FeCl₃·6H₂O), Iron(II) Chloride Tetrahydrate (FeCl₂·4H₂O), Hydrochloric acid (HCl) ammonium solution (NH₄OH) were used from BDH/England, Lead(II) Nitrate tetrahydrate (Pb(NO₃)₂), Copper(II) Nitrate (Cu(NO₃)₂), Cadmium(II) Nitrate ((Cd(NO₃)₂)) were used from Fluka/Switzerland.

Instruments: Thermal analysis was carried out using Thermal Gravimetry Analysis (TGA) (Perkin Elmer-TGA-4000) in College of Science, University of Muthanna at the heating rate 20°C/min in temperature range (40-605)

under nitrogen atmosphere with flow rate of 20 mL/min and Differential Scanning Calorimetric (DSC) analysis in College of Engineering, University of Tehran at the heating rate 10°C/min in temperature range (0-600) under nitrogen atmosphere. The Fourier Transform Infrared (FT-IR) spectra of the samples were recorded by (Shimadzu, Japan) in the Department of Chemistry College of Science, University of Thi-Qar by KBr disks, at ambient temperature. The surface morphology was examined from Scanning Electron Microscopy (SEM) and Transmission Electron Microscope (TEM) in College of Engineering, University of Tehran.

Nanomagnetic IPNs: The (epoxy resin-poly aniline) nanomagnetic semi IPNs were prepared by mixing (1 g) of nanomagnetic-polyaniline which were prepared by oxidation polymerization (Upadhyay *et al.*, 2016; Javidparvar *et al.*, 2016; Vivekanandan *et al.*, 2011) with (1 g) from the epoxy resins with weight ratio of (1:0.5) (Hafeez *et al.*, 2017; Siva *et al.*, 2014). Then heating using ultrasonic water bath at 50°C for 90 min to obtain a homogeneous mixture and kept in room temperature for 24 h. Then post cured 3h at 100°C.

Adsorption experiments (Khorshidi *et al.*, 2011; Rajeshwar Man Shrestha, 2015; Guclu *et al.*, 2007; Moradi *et al.*, 2012; Ata *et al.*, 2012; Perez-Marin *et al.*, 2007): The adsorption studies were carried out at 25°C. pH of the solution was adjusted to different values according to the requirement with different concentration of Hydrochloric acid (HCl) and ammonia solution. A known amount of different adsorbents was added to (Cu²⁺, Cd²⁺, Pb²⁺) samples separately and allowed sufficient time for adsorption equilibrium. The effects of various parameters on the rate of adsorption process were investigated by varying contact time, (10, 20, 30, 1, 2, 24) h, adsorbent amount (0.05 g) initial pH of the solution (2, 4, 6, 8), agitation speed (180 rpm) and temperature (25°C). The solution volume was kept constant 10 mL. After attaining the adsorption equilibrium all these mixtures were filtered. Filtrates were analyzed for (Cu²⁺, Cd²⁺, Pb²⁺) by flame atomic absorption spectrophotometer working at resonance wavelength (324.75, 228.8, 283.31) nm, respectively. The equilibrium adsorption capacity, q_e (mg/g) and the percentage removal of metal was calculated using the mass balance, according to the following Eq. 1:

$$q_e = (C_0 - C_e)V/m \quad (1)$$

Where:

V = The sample volume (L)

m = The mass of the adsorbents (g)

C₀ = The initial metal ion concentration (mg/L)

C_e = The equilibrium concentration of metal ion in the solution (mg/L)

The concentration of metal ions in the solution was determined with using atomic absorption spectrometer.

Study of adsorption isotherms: The 10 mL of four solutions with concentrations 1, 10, 20 and 30 ppm were prepared by proper dilution of stock solution of (Cu²⁺, Cd²⁺, Pb²⁺). The optimum conditions of pH, adsorbent dose, adsorbent particle size, agitation speed, temperature and contact time were adopted according to the sample of adsorbent used for studying adsorption isotherm. At the end, suspensions were filtered off and the filtrates were analyzed for remaining (Cu²⁺, Cd²⁺, Pb²⁺) concentration by using flame atomic absorption spectrophotometer. Langmuir isotherm was plotted by using its standard straight-line Eq. 2:

$$\frac{1}{q} = \frac{1}{bq_m C_e} + \frac{1}{q_m} \quad (2)$$

where, 'q' (mg g⁻¹) is the amount of metal ions adsorbed, 'C_e' (ppm) is the concentration of metal at equilibrium, q_m (mg g⁻¹) and b (L g⁻¹) are Langmuir isotherm parameters which were calculated from the slope and intercept values of the linear plot of 1/q versus 1/C_e. Freundlich isotherm was plotted using following standard straight-line Eq. 3:

$$\log q = \log K_F + \frac{1}{n} \log C_e \quad (3)$$

The value of K_F can be determined from intercept and 1/n can be determined from the slope of the linear plot of log q versus log C_e. K_F and 1/n are Freundlich isotherm parameters.

RESULTS AND DISCUSSION

Characterization

FTIR spectroscopy: Figure 1 shows the infrared spectrum of synthesized (NM semi IPNs). We have focused our attention on the vibrations of the epoxy ring of epoxy resin and amine group of PANI. The main characteristic of amine and hydroxide bands occur at 3100-3500 cm⁻¹. As these two absorptions are so close to one another, the net effect is that they merge into one vibration peak. In the curing process, a weak peak width of epoxide group and amine group is present which indicating the epoxide ring opening and cross linking process. This clearly shows the cross linking of epoxy resin by amine group present in the polyamine. On the other hand the, signatures of benzenoid and quinoid moieties of PANI are observed at 1508, 1464 cm⁻¹ (Siva *et al.*, 2014; Burkanudeen *et al.*,

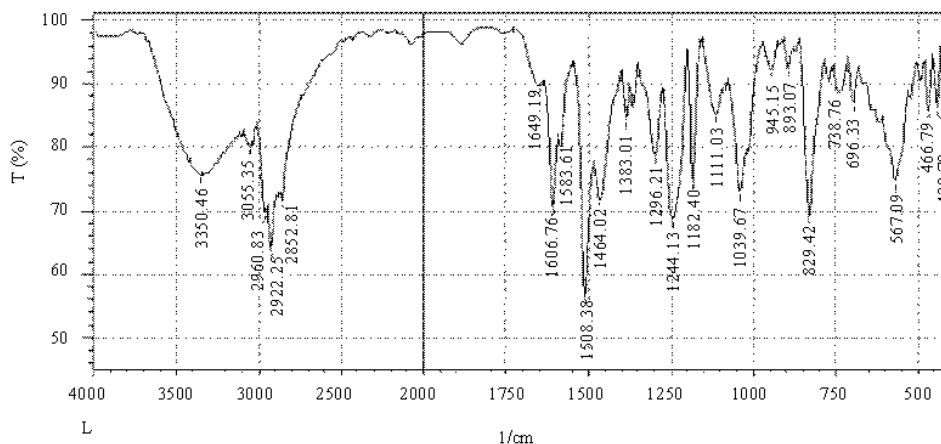


Fig. 1: FTIR spectra of (NM semi IPNs)

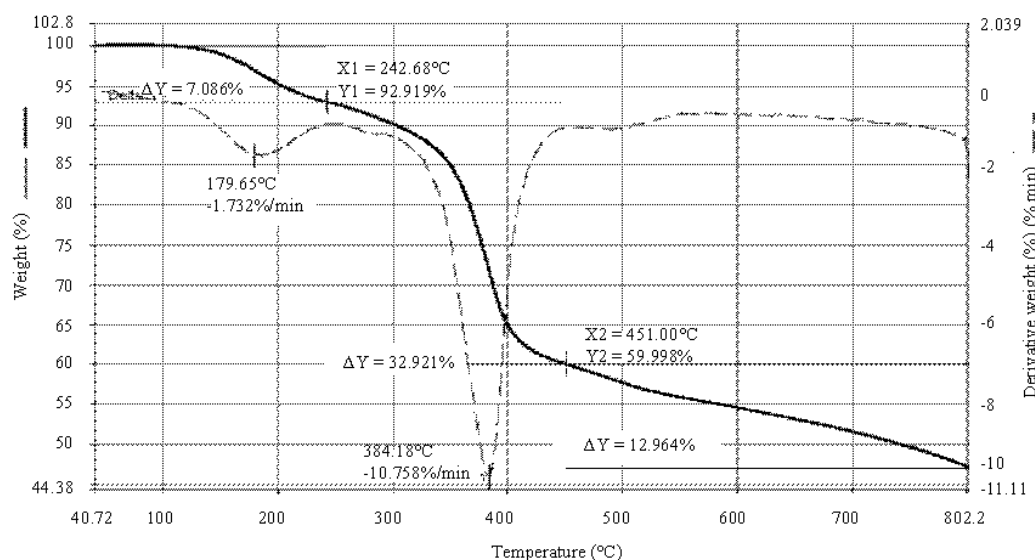


Fig. 2: TGA and DTG curves of (NM semi IPNs)

2010; Singru *et al.*, 2008). Also the vibration frequency of C = C stretching of aromatic group is found at 1606 cm^{-1} and peak at 567 cm^{-1} which is related to the vibration of Fe-O is also demonstrated in the Fig. 2 (Taty-Costodes *et al.*, 2003).

Thermal studies

Thermo Gravimetric Analysis (TGA) and Derivative Thermal Gravimetric (DTG) (Wei *et al.*, 2014; Asgari *et al.*, 2014; Birsan *et al.*, 2007): Thermal stability of (NM semi IPNs) was evaluated by Thermo Gravimetric Analysis (TGA) and Derivative Thermal Gravimetric (DTG) is shown in Fig. 2. Thermogram indicates that the three main stages of degradation, the first stage at below 250°C is related to the removal of absorbed moisture evaporation from matrix. The second stage around (250-455°C) is due to decomposition and

degradation the polymers on the surface of magnetic nanoparticles. The final temperature of decomposition is above 550°C. At higher temperature around (500-800°C), there is no significant change of weight. This implies that there is only iron oxide at this range of temperature.

Differential Scanning Calorimetric (DSC) analysis (Honmude *et al.*, 2012): The DSC thermograms of (NM semi IPNs) shown in Fig. 3 and showed that the endothermic peaks below 250°C attributed to the moisture evaporation while the endothermic curves above 250°C corresponds to the degradation of IPNs chain according to the TGA thermograms, on the other hand no T_m or T_g curves were showed in the DSC thermograms because the crosslink structure of nanomagnetic semi-interpenetrating polymer networks.

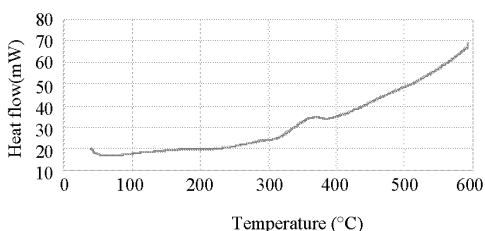


Fig. 3: DSC curve of (NM semi IPNs)

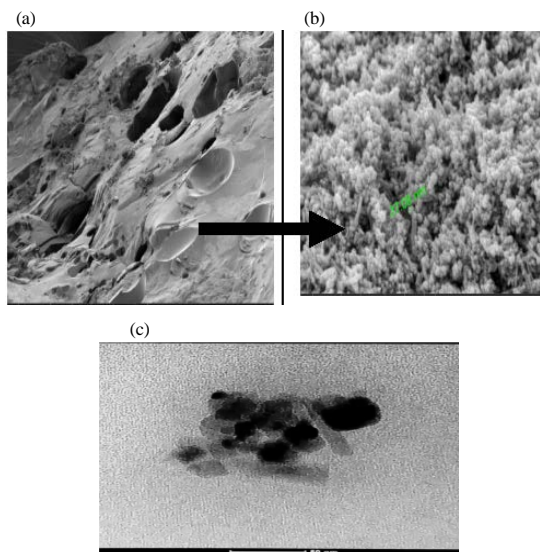


Fig. 4: a) SEM; b) TEM and c) OF (NM semi IPNs)

Surface morphology

Scanning Electron Microscopy (SEM) and Transmission Electron Microscopy (TEM): The size and morphology structure of (NM semi IPNs) were studied by Scanning Electronic Microscopy (SEM) and Transmission Electron Microscopy (TEM). It can be observed from Fig. 4 that, there are two distinct phases individual compound in network. AEP is porous and PANI nanorod dispersion within the epoxy matrix with diameter 37.08 nm which are in good agreement with the TEM results.

Analytical study

The effect of pH on removal metal ions: The pH value of the aqueous solution is an important controlling parameter in the adsorption process. These pH values influence the surface charge of adsorbent during adsorption. In order to assess the influence of this parameter on the adsorption, the experiments were carried out at different pH (2, 4, 6 and 8). The experiment was performed for (NM semi IPNs) studies with an initial concentration of 0.05 g at room temperature with different contact time for solutions from Cu(II), Cd(II) and Pb(II) ions. The effect of pH on the adsorption

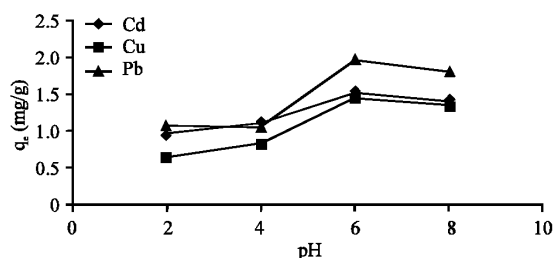


Fig. 5: Effect of pH on metals removal by (NM semi IPNs) at equilibrium time

capacity followed a similar trend (Fig. 5). At low pH values, the polymers exhibited a low adsorption capacity. This might be caused by two reasons, the competitive adsorption existed between the positively where there was an excess of H^+ ions in solution, a charged H^+ ions and the metal ions for the same active adsorptive sites which would result in the suppression of the metal ions adsorption onto the composite. On the other hand, at low pH values, the functions of polymers on surface were protonated which would cause a cationic repulsion between the metal ions and the active sites were protonated. As the pH increased, the composite surface became less positive due to the decrease of proton competitive adsorption and therefore ionic exchange and electrostatic attraction between the metal ions and the polymer were likely to be increased and pH above 6 maybe the metal ions are precipitate to form metal hydroxide (Atta *et al.*, 2015; Shrestha, 2015; Guclu *et al.*, 2007).

Effect of time: The equilibrium adsorption capacity of Cu^{+2} , Cd^{+2} and Pb^{+2} on surface (NM semi IPNs) as a function of contact time are shown in Fig. 5. The adsorption rate is rapid in the beginning due to more active sites available on polymer and gradually decreases until equilibrium state is reached due to occupancy of active sites of adsorbent (Shrestha, 2015; Guclu *et al.*, 2007; Marodi *et al.*, 2012).

Adsorption isotherms

(The Freundlich adsorption isotherm and Langmuir Isotherm) (Moradi *et al.*, 2012; Ata *et al.*, 2012; Perez-Marinet *et al.*, 2007): The adsorption studies were conducted by varying the initial metal ion concentrations 1, 10, 20 and 30 ppm with a constant dosage of adsorbent (0.05 g), optimum pH = 6 and optimum shaking time for capacity adsorption of all metal in this study. The Langmuir and Freundlich isotherms were shown graphically in Fig. 6-8 the corresponding parameters were listed in Table 1 and 2. According to the coefficients of

Table 1: Parameters of Freundlich and Langmuir constants for adsorption

Variables	Pb ²⁺	Cd ²⁺	Cu ²⁺
Freundlich isotherm parameters			
1/n	1.08	1.23	1.08
KF	0.49	0.527	0.752
R ² F	0.936	0.907	0.991
Langmuir isotherm parameters			
Q _m (mg g ⁻¹)	15.38	0.987	0.432
b (Lg ⁻¹)	0.011	0.133	0.016
R ² L	0.996	0.973	0.992

Table 2: Comparison of maximum adsorption capacity of (NM semi IPNs) with some other adsorbents

Adsorbent	Heavy metal	Q _{max} (mg g ⁻¹)	Source
Sawdust (pinus sylvestris)	Pb(II)	9.7800	60
Imperata cylindrica leaf	Pb(II)	13.500	61
Walnut sawdust	Pb(II)	4.4800	62
Sugarbeet pulp	Cu(II)	0.1500	63
Raw pomegranate peel	Cu (II)	1.3185	64
Sugarbeet pulp	Cu (II)	0.1500	65
Amberlite	Cd(II)	0.6400	66
polyaniline/polypyrrole nanoparticles			
Type 2		0.26100	67
Type 3		0.34500	
Type 4	Cd(II)	0.6390	
chromium doped nickel nanometal oxide	Cd(II)	0.1119	68

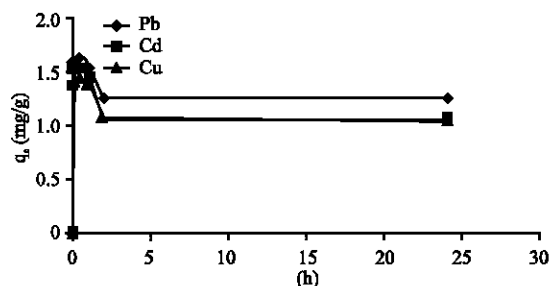


Fig. 6: Effect of contact time on metals removal by (NM semi IPNs) at pH = 6

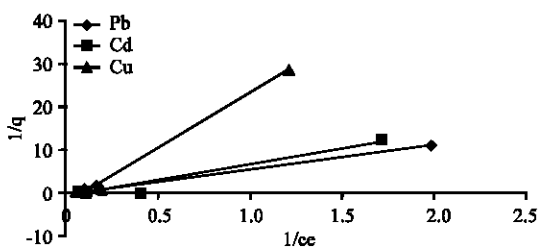


Fig. 7: Langmuir adsorption isotherm for metals adsorption by (NM semi IPNs) at pH = 6, shaking rate 180 rpm amount of adsorbent 0.05 g))

correlation obtained from linear regression, it was found that in all cases the Langmuir Model fit the data better than the Freundlich Model because the correlation coefficients (R^2) values are higher for Langmuir isotherm than for the Freundlich isotherm. This reinforces the fact

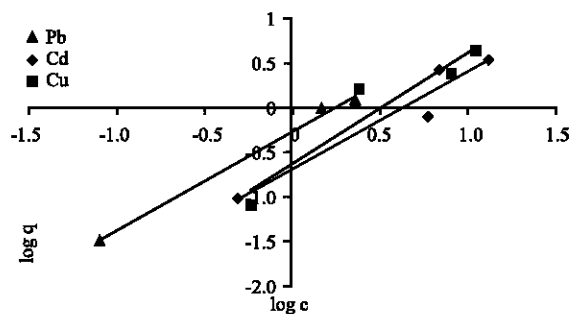


Fig. 8: Freundlich adsorption isotherm for metals adsorption by (NM semi IPNs) pH = 6, shaking rate 180 rpm amount of adsorbent 0.05 g))

that Langmuir isotherm is useful to explain the adsorption of all metals ions (Cu^{+2} , Cd^{+2} , Pb^{+2}) from the solutions on the surface (NM semi IPNs) are prepared in this study when it follows the monolayer mode rather than the multilayer mode. A basic assumption of the Langmuir theory is that the sorption can take place at specific homogeneous sites on the adsorption. When a site is occupied by an adsorbate no further adsorption can take place at that site.

CONCLUSION

This research reports, the synthesis of (NM semi IPNs) by sequential polymerization. TEM and SEM images showed the morphology of nanotube and spherical structure with well dispersed and excellent thermal stability. The (NM semi IPNs) has been investigated for the removal of different metal ions from aqueous solutions. The metals adsorption was tested at different conditions such as contact time and initial pH. The adsorption data followed Langmuir isotherm equation which indicated a monolayer adsorption.

REFERENCES

- Agarwal, K., M. Prasad, R.B. Sharma and D.K. Setua, 2011. Studies on microstructural and thermophysical properties of polymer nanocomposite based on polyphenylene oxide and Ferrimagnetic iron oxide. *Polym. Test.*, 30: 155-160.
- Asgari, S., Z. Fakhari and S. Berijani, 2014. Synthesis and characterization of Fe_3O_4 magnetic nanoparticles coated with carboxymethyl chitosan grafted sodium methacrylate. *J. Nanostruct.*, 4: 55-63.
- Ata, S., M. Imran Din, A. Rasool, I. Qasim and I. Ul Mohsin, 2012. Equilibrium, thermodynamics and kinetic sorption studies for the removal of coomassie brilliant blue on wheat bran as a low-cost adsorbent. *J. Anal. Methods. Chem.*, 2012: 1-8.

- Atta, A.M., A.M. El-Saeed, G.M. El-Mahdy and H.A. Al-Lohedan, 2015. Application of magnetite nano-hybrid epoxy as protective marine coatings for steel. *RSC. Adv.*, 5: 101923-101931.
- Birsan, C., D. Predoi and E. Andronescu, 2007. IR and thermal studies of iron oxide nanoparticles in a bioceramic matrix. *J. Optoelectron. Adv. Mater.*, 9: 1821-1824.
- Burkandeem, A., R. Azarudeen, M.R. Ahamed, P. Ramesh and N. Vijayan, 2010. Synthesis and analytical applications of a chelating resin. *Intl. J. Chem. Environ. Eng.*, 1: 29-34.
- Cristea, M., S. Ibanescu, C.N. Cascaval and D. Rosu, 2009. Dynamic mechanical analysis of polyurethane-epoxy interpenetrating polymer networks. *High Perform. Polym.*, 21: 608-623.
- Frisch, K.C., D. Klempner and H.L. Frisch, 1983. Recent advances in polymer alloys and IPN technology. *Mater. Des.*, 4: 821-827.
- Guclu, G., K. Guclu and S. Keles, 2007. Competitive removal of Nickel (II), Cobalt (II) and Zinc (II) ions from aqueous solutions by starch-graft-acrylic acid copolymers. *J. Appl. Polym. Sci.*, 106: 1800-1805.
- Hafeez, M., M. Faheem, Z. UAbdin, K. Ahmad and S. Fazil *et al.*, 2017. Synthesis and characterization of polyaniline-based conducting polymer and its anti-corrosion application. *Digest J. Nanomater. Biostructures*, 12: 707-717.
- Heath, J.R., 1999. Nanoscale materials. *Acc. Chem. Res.*, 32: 388-388.
- Honmote, S., S.V. Ganachari, R. Bhat, H.M.P. Kumar and D.S. Huh *et al.*, 2012. Studies on Polyaniline-Polyvinyl alcohol (PANI-PVA) Interpenetrating Polymer Network (IPN) thin films. *Intl. J. Sci. Res.*, 1: 102-106.
- Javidparvar, A.A., B. Ramezanzadeh and E. Ghasemi, 2016. The effect of surface morphology and treatment of Fe₃O₄ nanoparticles on the corrosion resistance of epoxy coating. *J. Taiwan Inst. Chem. Eng.*, 61: 356-366.
- Khorshidi, H.R., H. Eisazadeh and A.R. Khesali, 2011. Preparation and characterization of polyaniline containing Fe₃O₄ nanoparticles using sodium dodecylbenzenesulfonate as a surfactant. *High Perform. Polym.*, 23: 125-131.
- Moradi, O., B. Mirza, M. Norouzi and A. Fakhri, 2012. Removal of Co (II), Cu (II) and Pb (II) ions by polymer based 2-hydroxyethyl methacrylate: Thermodynamics and desorption studies. *Iran. J. Environ. Health Sci. Eng.*, 9: 1-9.
- Perez-Marin, A.B., V.M. Zapata, J.F. Ortuno, M. Aguilar and J. Saez *et al.*, 2007. Removal of cadmium from aqueous solutions by adsorption onto orange waste. *J. Hazard. Mater.*, 139: 122-131.
- Qin, C.L., D.Y. Zhao, X.D. Bai, X.G. Zhang and B. Zhang *et al.*, 2006. Vibration damping properties of gradient polyurethane/vinyl ester resin interpenetrating polymer network. *Mater. Chem. Phys.*, 97: 517-524.
- Radhakrishnan, S., C. Saujanya, P. Sonar, I.K. Gopalkrishnan and J.V. Yakhmi, 2001. Polymer-mediated synthesis of α -Fe₂O₃ nano-particles. *Polyhedron*, 20: 1489-1494.
- Ramis, X., A. Cadenato, J.M. Morancho and J.M. Salla, 2001. Polyurethane-unsaturated polyester interpenetrating polymer networks: Thermal and dynamic mechanical thermal behaviour. *Polym.*, 42: 9469-9479.
- Raymond, M.P. and V.T. Bui, 1998. Epoxy/castor oil graft interpenetrating polymer networks. *J. Appl. Polym. Sci.*, 70: 1649-1659.
- Shrestha, R.M., 2015. Removal of Cd (II) ions from aqueous solution by adsorption on activated carbon prepared from lapsi (*Choerospondias axillaris*) Seed Stone. *J. Inst. Eng.*, 11: 140-150.
- Singru, R.N., A.B. Zade and W.B. Gurnule, 2008. Synthesis, characterization and thermal degradation studies of copolymer resin derived from p-cresol, melamine and formaldehyde. *J. Appl. Polym. Sci.*, 109: 859-868.
- Siva, T., K. Kamaraj and S. Sathiyarayanan, 2014. Epoxy curing by polyaniline (PANI) Characterization and self-healing evaluation. *Prog. Org. Coat.*, 77: 1095-1103.
- Sperling, L.H. and V.B.A.T. Mishra, 1996. The current status of interpenetrating polymer networks. *Polym. Adv. Technol.*, 7: 197-208.
- Taty-Costodes, V.C., H. Fauduet, C. Porte and A. Delacroix, 2003. Removal of Cd(II) and Pb(II) ions, from aqueous solutions by adsorption onto sawdust of Pinus sylvestris. *J. Hazard. Mater.*, B105: 121-142.
- Tsumura, M., K. Ando, J. Kotani, M. Hiraishi and T. Iwahara, 1998. Silicon-based interpenetrating polymer networks (IPNs): Synthesis and properties. *Macromol.*, 31: 2716-2723.
- Unal, B., M.S. Toprak, Z. Durmus, H. Sozeri and A. Baykal, 2010. Synthesis, structural and conductivity characterization of alginate acid-Fe₃O₄ nanocomposite. *J. Nanopart. Res.*, 12: 3039-3048.
- Upadhyay, S., K. Parekh and B. Pandey, 2016. Influence of crystallite size on the magnetic properties of Fe₃O₄ nanoparticles. *J. Alloys Compd.*, 678: 478-485.

- Vivekanandan, J., V. Ponnusamy, A. Mahudewaran and P.S. Vijayanand, 2011. Synthesis, characterization and conductivity study of polyaniline prepared by chemical oxidative and electrochemical methods. *Arch. Appl. Sci. Res.*, 3: 147-153.
- Wei, W., X. Yue, Y. Zhou, Y. Wang and Z. Chen *et al.*, 2014. Novel ternary Fe₃O₄ polyaniline/polyazomethine/polyetheretherketone crosslinked hybrid membranes: Fabrication, thermal properties and electromagnetic behaviours. *Rsc.Adv.*, 4:11159-11167.
- Yu, X., G. Gao, J. Wang, F. Li and X. Tang, 1999. Damping materials based on polyurethane/polyacrylate IPNs: Dynamic mechanical spectroscopy, mechanical properties and multiphase morphology. *Polym. Intl.*, 48: 805-810.
- Yuhong, L., H. Huiming, W. Zhongyi, Z. Yaping and H. Jiang, 2010. Study on dental plastic IPN post composite. *J. Reinf. Plast. Compos.*, 29: 2684-2690.